International Journal of Control
Publication details, including instructions for authors and subscription information:
http://www.tandfonline.com/loi/tcon20

Robust control of dynamically interacting systems

J. E. COLGATE [a] & N. HOGAN [a]
[a] Department of Mechanical Engineering , Massachusetts Institute of Technology , Cambridge, MA, 02139, U.S.A.
Published online: 29 Oct 2007.

To cite this article: J. E. COLGATE & N. HOGAN (1988) Robust control of dynamically interacting systems, International Journal of Control, 48:1, 65-88, DOI: 10.1080/00207178808906161

To link to this article: http://dx.doi.org/10.1080/00207178808906161

INT. J. CONTROL, 1988, VOL. 48, NO. 1, 65–88

Robust control of dynamically interacting systems

J. E. COLGATE† and N. HOGAN†

Dynamic interaction with the environment is fundamental to the process of manipulation. This paper describes an approach to the design of 'interaction controllers' and contrasts this with an approach to servo design. The need for 'coupled stability' and 'interactive behaviour' specifications is motivated. A necessary and sufficient condition to ensure the stability of a linear manipulator coupled at a single interaction port to a linear, passive environment is found. It is shown that this condition may be extended to a broad class of active environments, and a simple test for coupled stability, based on the root locus, is presented. Two interaction controller designs for a linear manipulator are presented. Interactive behaviour is analysed in the frequency domain by comparison with the behaviour of a target model. A simple controller shows strong stability properties, but poor behaviour; a more sophisticated design shows that it is possible to achieve desirable behaviour while retaining stability guarantees.

1. Introduction

The study of manipulation, both human and machine, provides a strong incentive for understanding the control of interacting systems. Interaction—the exchange of mechanical work—is fundamental to the process of manipulation. The human arm is an exemplary manipulator, capable of interacting in a well-behaved manner with an extremely diverse set of environments. Its repertoire includes the ability to position and move an eating utensil stably, to perform complex dynamic tasks such as catching or throwing a ball, and to perform kinematically constrained tasks such as sanding a surface or opening a drawer.

This tiny selection of tasks in fact encompasses a far broader range than that achievable by a mechanical manipulator controlled with state-of-the-art servo (i.e. command-following) techniques. Most successful industrial applications of robots have been in non-contact applications such as spray-painting or welding, or in simple pick-and-place operations. However, the bulk of industrial operations to which a robot might be applied require significant work transfer. These operations include drilling, reaming, counter boring, grinding, bending, and chipping (Hogan 1985 a).

The future undoubtedly holds more tasks for which interaction is essential. One of the more interesting is that of two or more robots working together, perhaps on an assembly task. In this example, the conventional strategy of making the robot much 'stiffer' than the environment (to 'reject' environmental disturbances' is bound to encounter difficulties—the environment is just another, perhaps identical, robot.

It is also alluring to envisage robots catching and, perhaps, throwing workpieces. This is not as unrealistic as it may seem, and it is a technique that humans have taken advantage of in a number of real assembly operations. Also of interest are mobile and underwater robots which need to manipulate the environment successfully without the aid of a firm base.

Received 13 July 1987.

† Department of Mechanical Engineering, Massachusetts Institute of Technology, Cambridge, MA 02139, U.S.A.

These examples suggest that a better understanding of the control of interacting systems, and of the success of the human arm, is pertinent to efforts at increasing the flexibility and expanding the repertoire of robotic manipulators. However, while manipulation is currently the primary concern, an approach to the problem of responding to significant environmental disturbances is appropriate to virtually every branch of control. For this reason, an attempt will be made in this paper to make the least restrictive sets of assumptions possible with regard to the specific nature of the interacting systems.

2. Design goals

Design specifications for a servo controller may be stated in virtually any manner the designer chooses, but they generally include some subset of those shown in Fig. 1.

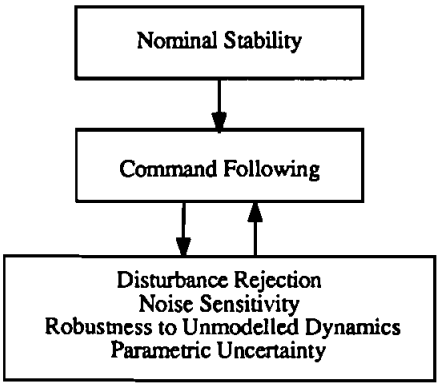

Figure 1. Design specifications for a servo.

The general hierarchy is as shown in this figure. Nominal stability is, of course, an absolute requirement, while trade-offs are required for the other specifications. A linear system (such as that shown in Fig. 2) offers a quantitative example. One manner in which frequency domain specifications may be chosen (Lehtomaki 1981) uses the layout shown in Fig. 2 and the following notation:

- $K(s)$ forward path compensator
- Φ, B, C represent the plant
- $M(s)$ frequency-dependent bound on the modelling errors (reflected at the plant output)
- $r(s)$ reference signal that $y(s)$ is to follow
- $d(s)$ disturbance
- $n(s)$ noise input

We define

$$T(s) = C\Phi(s)BK(s)$$

$$S(s) = [I + T(s)]^{-1}$$

$$C(s) = [I + T(s)]^{-1}T(s)$$

Let ω_b be the desired control bandwidth, ω_d the bandwidth in which disturbances

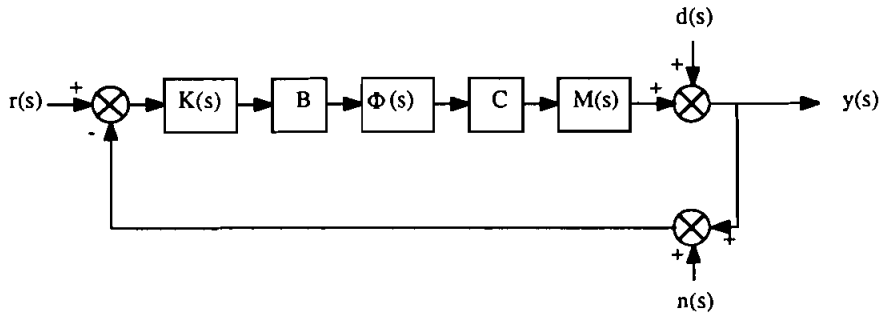

Figure 2. Servo structure.

contain significant energy, ω_p the greater of ω_b and ω_d, and δ a design value such that $0 < \delta \ll 1$.

Then we have the following properties.

Nominal stability

The poles of $C(s)$ must lie in the left half s-plane (LHP).

Command following

$1 - \delta \leqslant \sigma_{min} C(j\omega) \leqslant \sigma_{max} C(j\omega) \leqslant 1 + \delta$ for $\omega < \omega_p$, where σ_{min} and σ_{max} are the minimum and maximum singular values of the matrix argument (in this case, $C(j\omega)$), respectively.

Disturbance rejection and noise sensitivity

$\sigma_{max} S(j\omega) \leqslant \delta$ for $\omega < \omega_p$.

Robustness

$\sigma_{max}[M(j\omega) - I] < \sigma_{min}[C^{-1}(j\omega)]$ for all ω.

It is important to stress that these are not the only design specifications that may be used in designing a controller for the system in Fig. 2, nor even necessarily the best (note that robustness to parameter uncertainty is omitted). They are, however, representative of a well-conceived approach to servo design.

The design specifications for an 'interaction controller' will be somewhat different. The hierarchical structure is shown in Fig. 3. Stability of the isolated system remains paramount; however, as a manipulator is expected to interact extensively with its environment, coupled stability is nearly as important. Coupled stability may, however, be traded off against performance; a manipulator need not be capable of interacting stably with every conceivable environment, just those which it is likely to encounter. Interactive behaviour has been added to the performance specifications since stability is clearly an insufficient requirement; reasonable behaviour is also required. The other requirements are essentially as before; however, in this introductory paper we concern ourselves with only the top three levels of this hierarchy.

A linear system (Fig. 4) provides a quantitative illustration of these specifications. All notation is as in Fig. 2, except that $E(s)$ represents the driving-point impedance of

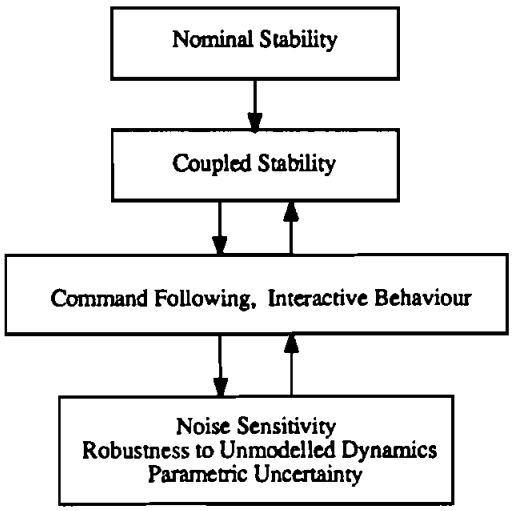

Figure 3. Design specifications for an interaction controller.

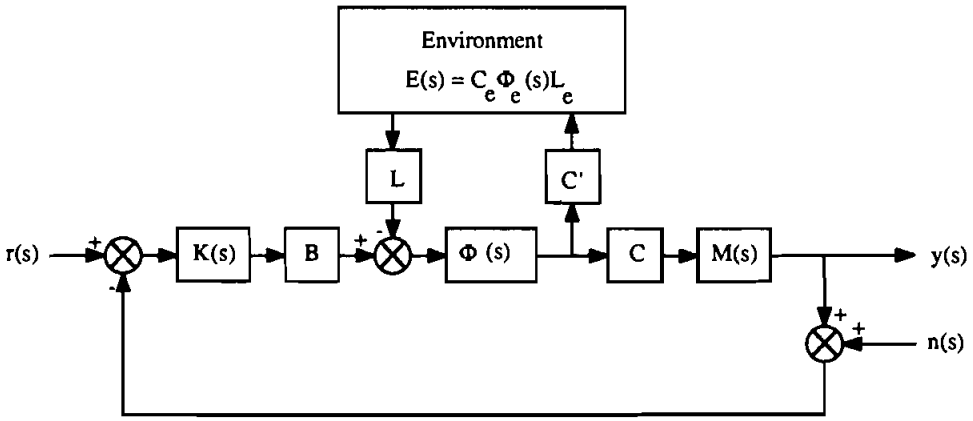

Figure 4. Interaction controller structure.

any linear, passive environment with which the manipulator may couple (assuming a passive environment eliminates the difficulty of unstable environments; we elaborate on this later). L and C' represent the input–output coupling of the manipulator to this environment. $T(s)$, $S(s)$, $C(s)$, ω_b, and δ are as defined previously. In addition, $Q(s)$ is defined as

$$Q(s) = [I + \{LE(s)C' + BK(s)C\}\Phi(s)]^{-1}\Phi(s)$$

$Q(s)$ contains the dynamics of the entire coupled system.

One method of establishing specifications is to choose a target system which has the desired performance, in terms of both command following and interactive behaviour. This would require the selection of the matrices B_t, $\Phi_t(s)$, C_t, L_t, and C'_t. Then the specifications could be stated as follows.

Nominal stability

The poles of $C(s)$ must lie in the LHP.

Coupled stability

The poles of $Q(s)$ must lie in the LHP for any possible $E(s)$.

Command following

$$\text{Abs}\,[\sigma_{\max}\{C(j\omega)\} - \sigma_{\max}\{C_t\Phi_t(j\omega)B_t\}] \leqslant \delta \quad \text{for } \omega < \omega_b$$
$$\text{Abs}\,[\sigma_{\min}\{C(j\omega)\} - \sigma_{\min}\{C_t\Phi_t(j\omega)B_t\}] \leqslant \delta \quad \text{for } \omega \leqslant \omega_b$$

Interactive behaviour:

Let $Q_t(s) = [I + L_t E(s) C_t \Phi_t(s)]^{-1} \Phi_t(s)$, then

$$\text{Abs}\,[\sigma_{\max}(Q(j\omega)\} - \sigma_{\max}\{Q_t(j\omega)\}] \leqslant \delta \quad \text{for } \omega \leqslant \omega_b$$
$$\text{Abs}\,[\sigma_{\min}\{Q(j\omega)\} - \sigma_{\min}\{Q_t(j\omega)\}] \leqslant \delta \quad \text{for } \omega \leqslant \omega_b$$

Specifications for noise sensitivity and robustness may be added at a later date.

The most striking difference between these specifications and those for the servo is the way in which environmental 'disturbances' are treated. As a consequence of treating the environment as a dynamic system which, when coupled, affects the dynamics of the manipulator, two new specifications show up; guaranteeing stability and reasonable behaviour evidently becomes a more demanding proposition.

The point of this section has been to illustrate clearly that 'interaction control' embraces a philosophically different approach to controller design, as manifested in the sets of design specifications. One of the primary goals of this research is to demonstrate that this is more than a simple change in viewpoint, that different controller designs and performance result.

As a final note, it will be emphasized again that neither of the sets of linear design specifications is unique, or even the best choice; both sets, however, are representative of well-conceived design approaches.

3. Impedance control

The concept of active control of a manipulator's interactive behaviour is formally treated as an aspect of 'impedance control' (Hogan 1985 a, b, c). Impedance control is an approach to manipulation based on the assertion that it is not sufficient to control some vector of port variables such as positions, velocities or forces, but that it is also necessary to control the dynamic relations among the port variables, such as impedances and admittances†. In particular, impedance control makes the reasonable assumption that most environments a manipulator will interact with are admittances (i.e. kinematic constraints or mass-like objects), and that to be causally consistent, the port behaviour of the manipulator should be that of an impedance. To illustrate, a

† Note that although the terms impedance and admittance are commonly restricted to linear systems, they may be applied to non-linear systems as well. They are causal dynamic operators which map an input time function $\mathbf{u}(t)$ onto an output time function $\mathbf{y}(t)$ such that the present value of the output $\mathbf{y}(t)$ may depend on the entire past history of the input $\mathbf{u}(t-\tau)$ for $0 < \tau < \infty$ (Paynter 1961).

single-axis manipulator connected to an admittance-type environment may be represented by the bond graph shown in Fig. 5. The job of the impedance controller is to modulate both v_0, the 'virtual trajectory' of the manipulator (Hogan 1985 a), and Z, the manipulator impedance.

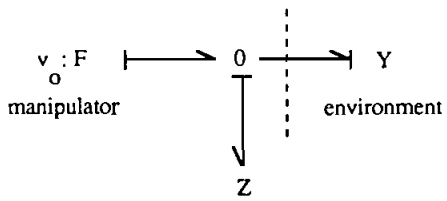

Figure 5. Bond graph representation of an impedance controlled manipulator.

As an aside, the postulate of 'physical equivalence' has been employed in using a bond graph to represent a controlled manipulator. Physical equivalence states: 'It is impossible to devise a controller which will cause a physical system to present an apparent behaviour to its environment which is distinguishable from that of a purely physical system' (Hogan 1985 a). This postulate allows the use of a physical systems modelling technique—bond graphing—to describe a controlled manipulator.

Hogan has shown (1985 a) that a large class of non-linear, multi-axis manipulators may be represented by the structure in Fig. 5. He has also shown, in a few cases (1985 b), how an impedance controller may be designed. The benefits of these designs are also well documented (Hogan 1984, 1985 d). The design methods offered do not, however, apply to a broad range of manipulators. Indeed, impedance control is intended to provide an approach to understanding manipulation rather than a prescription for designing controllers.

The work presented in this paper may be classed as impedance control. It should be evident that the use of a design specification for command-following and one for interactive behaviour is simply a restatement of Hogan's assertion that both a vector of port variables and the port impedances must be controlled. This work is, however, an attempt to formulate the problem in a manner that is well suited to the design of interaction controllers for a broad range of manipulator (and other) models.

4. Controller structure

The structure of the 'complete system' to be studied in this paper is shown in Fig. 6. It consists of an active system (the manipulator) with m states, n control ports, and p interaction ports (generally, $m \geqslant n \geqslant p$), connected at the appropriate ports to a controller and a passive environment.

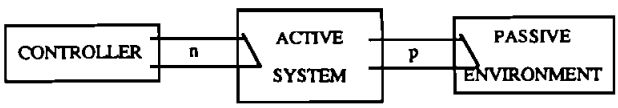

Figure 6. Structure of manipulator/environment system.

We assume that the control may be divided into a state-dependent part and a state-independent part, i.e. that the control vector $\mathbf{u}$ may be expressed as $\mathbf{u} = \mathbf{h} + \mathbf{r}$, where $\mathbf{h}$ is the output of a compensator whose inputs are the states of the active

system, and **r** represents the state-independent control, which itself may be the output of a dynamic system. The complete system may now be reconfigured as shown in Fig. 7.

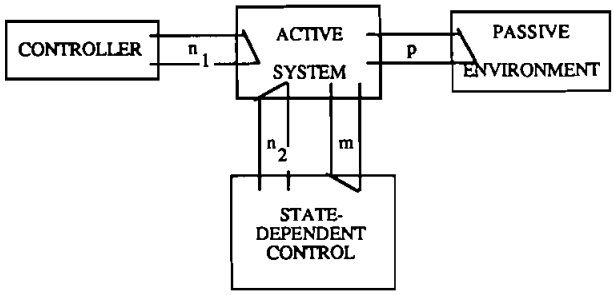

Figure 7. Structure of manipulator/environment system; control divided into state-dependent and state-independent parts.

At this point, it is worth elaborating on the restriction to passive environments. This restriction may be justified simply on the basis that many environments of interest are passive. These include inertial loads such as parts for palletizing or assembly, and kinematic constraints such as crank handles or surfaces to be ground. However, many environments, such as power tools and other manipulators, are active. Yet, in many cases, these environments may be analysed in the same way as strictly passive environments. This is demonstrated in the next section.

Finally, a change in viewpoint will be made. The combination of the active system and state-dependent control will be viewed as a controlled network, as shown in Fig. 8. The value of this viewpoint is that it indicates that the wealth of literature and experience in the area of network analysis and synthesis may be applied to the problem of controlling interaction. For instance, it is shown in the next section that, for the linear case, if the interaction port impedance of the controlled network has the properties of a positive real function, the network will remain stable when coupled to any passive environment. The concept of a positive real function is borrowed directly from network theory.

Figure 8. Network representation of manipulator/environment system.

5. Coupled stability

This section consists of an informal proof that a linear system must have a positive real driving point impedance (the properties of a positive real function are described in Appendix A) at any port where it couples to a passive linear environment if the coupled system is to be guaranteed stable. Certain interesting corollaries of this proof are also presented.

Consider two linear, time-invariant networks, each with an open interaction port as shown in Fig. 9. We are interested in the stability of the system that results when these two networks are coupled along their interaction ports, i.e. the stability of the system

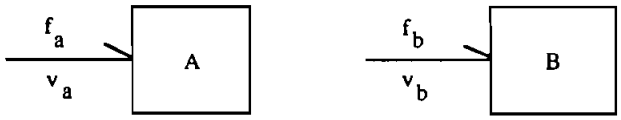

Figure 9.

shown in Fig. 10. (Alternatively, these systems could be coupled with a 0-junction, in which case $f_a = f_b$ and $v_a = -v_b$, however, the stability result would be unaffected. See Rosenberg and Karnopp 1983 for an explanation of 0- and 1-junctions.)

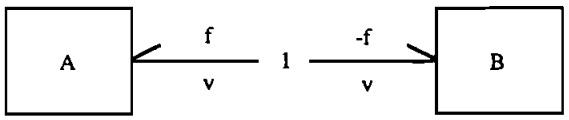

Figure 10.

Figure 10 may be rewritten in the block diagram form shown in Fig. 11. Implicit in this representation is the linear nature of A and B, i.e. both $A(s)$ and $B(s)$ may be expressed as the ratio of two rational polynomials in s.

The dynamics of the coupled system are

$$\mathbf{0} = \begin{bmatrix} -1 & B(s) \\ -A(s) & -1 \end{bmatrix} \begin{bmatrix} v(s) \\ f(s) \end{bmatrix} \tag{5.1}$$

In order that a stable solution exist, the roots of the characteristic equation, $1 + A(s)B(s)$, must fall on the imaginary axis or within the LHP.

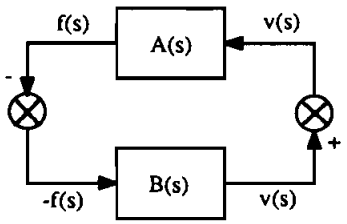

Figure 11.

A Nyquist procedure may be used to study the pole locations. The basis of the Nyquist procedure is the use of the principle of the argument and of a well-chosen mapping between complex planes. The principle of the argument is as follows.

'The number of clockwise encirclements of the origin by a map of $G(s)$ of a clockwise contour in the s-plane equals the number of zeros of G within the contour minus the number of poles of G within the contour.'

A counterclockwise encirclement counts as -1 clockwise encirclements. Generally, the transfer function of interest is $1 + G(s)$, which is the quotient of open-loop and closed-loop (unity feedback) characteristic polynomials. Rather than map through $1 + G(s)$,

however, it is convenient to map through $G(s)$ and investigate encirclements of the -1 point.

Next, the Nyquist contour is chosen. As indicated in Fig. 12, this contour includes the entire closed RHP, but excludes any poles on the imaginary axis. An example of the mapping in the $G(s)$ plane is also shown in Fig. 12. This mapping is necessarily symmetric about the real axis as $G(s)$ may be written as a ratio of two polynomials in s, $N(s)/D(s)$, the real part of which is an even function of ω on the $j\omega$ axis, and the imaginary part of which is an odd function. The behaviour very near a pole on the $j\omega$ axis or as $R \to \infty$ is determined by the dominant pole (or poles, if they are not simple). Thus, an arc of 180° in the s-plane, taken at an infinitesimal radius around a pole on the $j\omega$ axis or at ∞, and starting at $\pm 90°$, must result in an arc in the $G(s)$ plane that is some multiple of 180°, and is symmetric about the real axis.

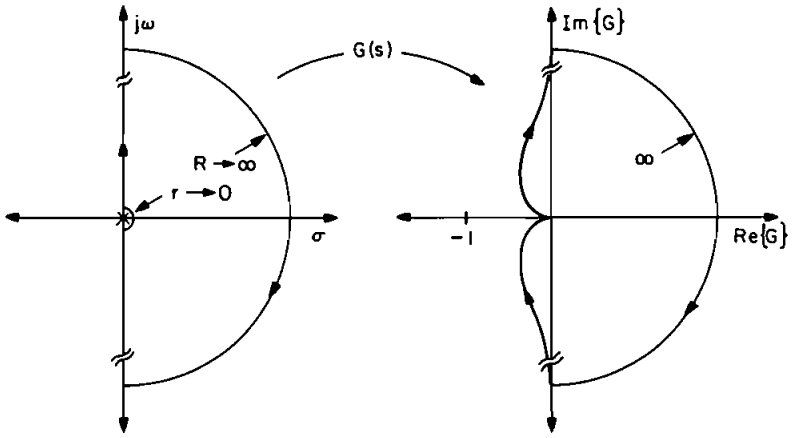

Figure 12. Example of a mapping of the Nyquist contour.

Once the mapping through $G(s)$ has been generated, it is a simple matter to interpret the principle of the argument as follows.

'The number of clockwise encirclements of the -1 point by a mapping through $G(s)$ of the Nyquist contour equals the number of unstable closed loop (unity feedback) poles within the contour minus the number of unstable open-loop poles (i.e. of $G(s)$) within the contour.'

As we are interested in the roots of $1 + A(s)B(s)$, we should replace $G(s)$ with $A(s)B(s)$ in the analysis above. Some further assumptions about $A(s)$ and $B(s)$ are now necessary. First, $A(s)$ is identified with our controlled system, and $B(s)$ is identified with the environment.

Next, assume that the input and output of $A(s)$ have been chosen appropriately so that a state space realization exists; i.e. so that F_a, G_a, H_a and J_a exist which satisfy

$$\begin{aligned} \dot{\mathbf{x}} &= F_a\mathbf{x} + G_a v \\ f &= H_a\mathbf{x} + J_a v \end{aligned} \tag{5.2}$$

and

$$A(s) = J_a + H_a(sI - F_a)^{-1}G_a \tag{5.3}$$

This is equivalent to requiring that $A(\infty) < \infty$. Further, assume that the eigenvalues of F_n lie in the closed LHP. These assumptions, taken together, guarantee that the poles of $A(s)$ lie in the closed LHP, and are indicative of a stable system.

Finally, the environment is restricted to be linear and passive. As a consequence of representing the driving point impedance of a passive system, $B(s)$ is a positive real function, and as such has the property that $\mathrm{Re}\{B(s)\} \geqslant 0$ for $\mathrm{Re}\{s\} \geqslant 0$ (see Appendix A). Thus, a mapping of the Nyquist contour through $B(s)$ alone yields a curve which must lie wholly within the RHP or on the imaginary axis. In fact, a mapping of the Nyquist contour through all possible positive real functions (passive two terminal networks) simply yields the entire closed right-half $B(s)$ plane.

If $B(s)$ is viewed as a compensator which affects the magnitude and phase of $A(s)$, then the class of all such compensators will include those capable of altering the phase by $\pm 90°$ and changing the magnitude by a factor of 0 to ∞. Therefore, it is clear that, in order to interact stably with all passive environments, $A(s)$ must have a phase margin of $\pm 90°$, an upward gain margin of ∞, and a downward gain margin of 0.

The effect of these restrictions is to limit mappings of the Nyquist contour through $A(s)$ to lie in the closed right half $A(s)$-plane. For any path that enters the LHP in a clockwise fashion, no more than 90° additional lead or lag will be necessary to cause the path to cross the negative real axis, and, once crossing the axis, some gain between 0 and ∞ will cause the path to encircle the -1 point. An example of this is illustrated in Fig. 13 (*a*); the Nyquist plots shown in Figs. 13 (*b*) and 13 (*c*) are clearly

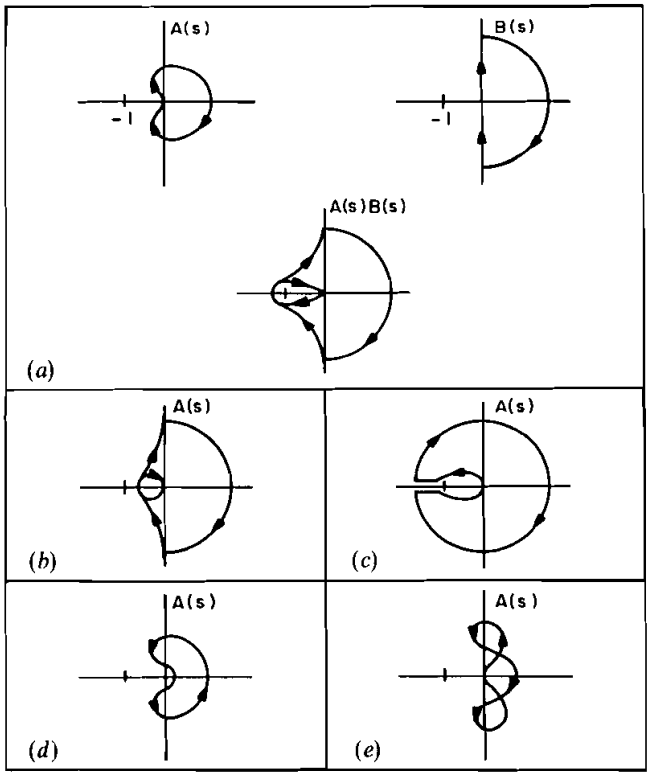

Figure 13. Nyquist plots of systems which fail to satisfy the coupled stability criterion.

inadmissible for the same reason. The Nyquist plots shown in Figs. 13 (*d*) and 13 (*e*), however, enter the LHP in a counterclockwise fashion, and will not be reshaped by any acceptable $B(s)$ to yield a clockwise encirclement of the origin. It may be shown, however (see Appendix B) that any Nyquist plot which contains a counterclockwise loop is indicative of an RHP pole, violating one of our previous assumptions.

Thus, the mapping through $A(s)$, like that through $B(s)$, is restricted to lie wholly within the closed RHP. This is a necessary condition to ensure coupled stability, and is a necessary and sufficient condition for $A(s)$ to represent the driving point impedance of a passive network (Brune 1931). Because the energy of this passive network may be selected as a Lyapunov function, it is clear (following the arguments of Fasse 1987) that we also have a sufficient condition for stability when coupled to any passive environment, linear or non-linear, that is describable in hamiltonian (or lagrangian) form. In conclusion, $A(s)$ being positive real is a necessary and sufficient condition to ensure stability when coupled to any passive, hamiltonian environment. □

This completes the proof, but there are a number of related ideas which are useful.

Coupling of active systems

It is possible to extend this stability result to include active linear systems provided that the active terms are not state-dependent. Figure 14 demonstrates how an active term may be added. It is evident that this active term has no effect on the stability of the loop unless u is in some way state-dependent. In fact, both A and B may be active without jeopardizing stable coupling if both satisfy the positive real condition when the state-independent control is turned off.

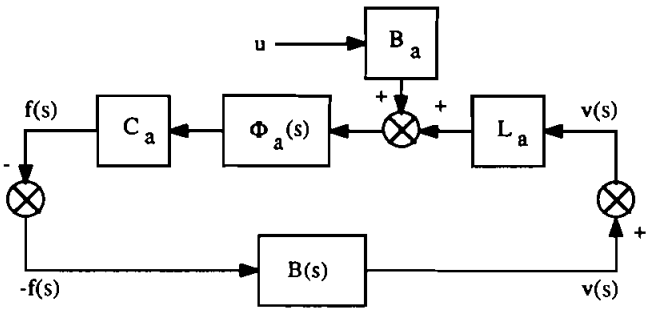

Figure 14. Coupling of an active system to a passive system.

'Worst' environment

As will be evident in the next section, explicitly enforcing the positive real condition in a control system may become mathematically cumbersome. For this reason, an analytical tool that provides a simple test for positive realness would be useful. The choice of a 'worst' (most destabilizing) environment is one such tool.

For any $A(s)$, positive real or not, the passive environment that is the most destabilizing may be defined as that which tailors the shape of the Nyquist plot of $A(s)B(s)$ so as to minimize the radius of a circle centred at the -1 point and which just touches the Nyquist plot. If the radius of this circle may be made to go to zero, however, the coupled system is unstable and any further pure rotation of the Nyquist plot will not change this.

Thus, it seems sensible, in the search for the 'worst' passive environment, to restrict oneself to only those whose Nyquist plots lie wholly on the imaginary axis, thus providing the maximum rotation. These are the Nyquist plots of lossless systems, such as pure masses and pure springs whose driving point impedances always have the form of a/s or as.

Therefore, for any $A(s)$, the worst environment may be found in the set of all pure masses and springs. Of course, the most stabilizing environment is also some pure mass or spring, as one of these provides the maximum rotation away from the negative real axis.

In general there will be a particular set of springs or masses which contains the worst environments for a given system. One way to find this set is to search the entire space. This is not as difficult as it may seem, being simply a version of the root locus.

Consider, for instance, the case in which $A(s)$ is an admittance and the worst environment is some spring k_e or mass M_e. Coupling $A(s)$ to the spring results in the system shown in Fig. 15. We can investigate the stability of this system for all spring constants just by generating a root locus for the plant, $(1/s)A(s)$. We can similarly investigate the stability of the system for all masses by replacing the plant with $sA(s)$, and the gain by M_e.

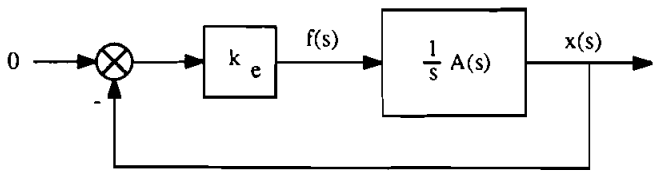

Figure 15. Coupling of system A to a spring.

6. Stable coupling—A linear example

The purpose of this section is to demonstrate that, given a particular control law, the positive real condition may be enforced to guarantee coupled stability.

The linear system that will be used for the analyses in both this section and § 7 is shown in Fig. 16. This system is a crude linear representation of a manipulator. The spring k_2, the damper b_2 and the mass M_2 represent, roughly, the 'hardware' dynamics, i.e. factors such as flexibility and friction at the joints and link inertias. The damper b_1 and the mass M_1, on which the control E acts, represent actuator dynamics, and the spring k_2 represents transmission dynamics. F represents forces imposed by the environment. This model, while crude, will prove to be representative of some of the difficulties of controlling the interactive behaviour of a manipulator which has significant actuator and transmission dynamics.

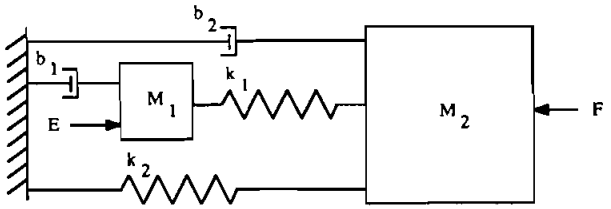

Figure 16. Linear manipulator.

The state equations of this manipulator are:

$$\frac{d}{dt}\begin{bmatrix} x_1 \\ x_2 \\ v_1 \\ v_2 \end{bmatrix} = \begin{bmatrix} 0 & 0 & 1 & 0 \\ 0 & 0 & 0 & 1 \\ -k_1/M_1 & k_1/M_1 & -b_1/M_1 & 0 \\ k_1/M_2 & -(k_1+k_2)/M_2 & 0 & -b_2/M_2 \end{bmatrix} \times \begin{bmatrix} x_1 \\ x_2 \\ v_1 \\ v_2 \end{bmatrix} + \begin{bmatrix} 0 \\ 0 \\ 1/M_1 \\ 0 \end{bmatrix} E + \begin{bmatrix} 0 \\ 0 \\ 0 \\ 1/M_2 \end{bmatrix} F \tag{6.1}$$

where x_1 and v_1 refer to the position and velocity of M_1, and x_2 and v_2 refer to M_2.

For this section, the following control law (motivated by an impedance control law for an inertial manipulator (Hogan 1985 b) will be used

$$E = -K(x_2 - x_0) - B(v_2 - v_0) \tag{6.2}$$

Were it not for actuator and transmission dynamics (i.e. if E acted directly on M_2), the effect of this control law would be to adjust the stiffness and damping coefficients of the manipulator hardware, and to introduce x_0 and v_0 which would act as the 'virtual trajectory' (Hogan 1985 a). However, as will be demonstrated, this is not the actual effect.

We are interested in controlling the interactive behaviour of this system expressed in the driving point admittance, relating force input to velocity output, i.e. $v_2(s)/F(s)$. If the poles of this function lie in the LHP, then the system is stable when uncoupled (assuming no pole-zero cancellations in the RHP), and if this function is positive real, then the system is stable when coupled to any passive linear environment (also assuming no pole-zero cancellations in the RHP). Although the algebra becomes somewhat involved, inequality constraints which limit the values of K and B to those that lead to a result satisfying the uncoupled and coupled stability requirements may be found. The results are

$$D(s) = M_1 M_2 s^4 + (b_1 M_2 + b_2 M_1)s^3 + (b_1 b_2 + k_1 M_1 + k_2 M_1 + k_1 M_2)s^2 + (b_1(k_1 + k_2) + k_1(b_2 + B))s + k_1(k_2 + K) \tag{6.3}$$

$$\frac{v_2(s)}{F(s)} = \frac{s(M_1 s^2 + b_1 s + k_1)}{D(s)} \tag{6.4}$$

For uncoupled stability:

(1) $$-b_2 - b_1\left[\frac{k_1 + k_2}{k_1}\right] \leqslant B \leqslant \frac{b_1^2 b_2}{k_1 M_1} + \frac{b_1 b_2^2}{K_1 M_2} + \frac{b_1 M_2}{M_1} + \frac{b_2 M_1(k_1 + k_2)}{k_1 M_2} \tag{6.5}$$

(2) $$K \geqslant -k_2 \tag{6.6}$$

(3) $$K \leqslant \frac{\alpha_1(B)\alpha_2(B)}{\alpha_3} - k_2 \tag{6.7}$$

where

$$\alpha_1(B) = b_1(k_1 + k_2) + k_1(b_2 + B)$$

$$\alpha_2(B) = b_1^2 b_2 M_2 + b_1 b_2^2 M_1 + b_1 k_1 M_2^2 + b_2 M_1^2(k_1 + k_2) - k_1 M_1 M_2 B$$

$$\alpha_3(B) = k_1(b_1 M_2 + b_2 M_1)^2$$

For coupled stability:

(4) $$k_1^2(b_1 + b_2 + B) - b_1 K^2 \geqslant 0 \tag{6.8}$$

(5) while

$$\beta(B) = b_1^2 b_2 - b_2 k_1 M_1 - k_1 M_1(b_2 + B) \leqslant 0$$

then

$$\beta^2(B) - 4b_2 M_1^2\{k_1^2(b_1 + b_2 + B) - b_1 k_1 K\} \leqslant 0 \tag{6.9}$$

Figure 17 is a graphical representation of these inequalities given the following parameter values

$$b_1 = 4{\cdot}8 \quad b_2 = 6{\cdot}0$$

$$k_1 = 160{\cdot}0 \quad k_2 = 100{\cdot}0$$

$$M_1 = 0{\cdot}1 \quad M_2 = 1{\cdot}0$$

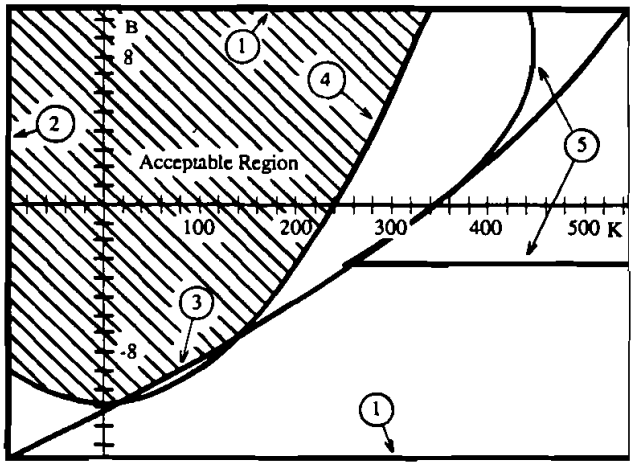

Figure 17. Feedback gains which yield coupled and uncoupled stability. Numbers refer to the inequality constraints in the text.

As a concrete example of a design process, consider the target system shown in Fig. 18 which embodies the desired behaviour of our manipulator, where $b_0 = 4{\cdot}24$, $k_0 = 9{\cdot}0$, and $M_0 = 1{\cdot}0$. These parameters correspond to a considerably more compliant system than the uncontrolled manipulator—it is not always desirable in the case of manipulation to generate very high stiffnesses as a servo typically does.

One technique for choosing K and B is to ignore the actuator and transmission dynamics of the manipulator, in which case (since $M_2 = M_0$) the very simple conditions $k_2 + K = k_0$ and $b_2 + B = b_0$ appear to generate the target system exactly.

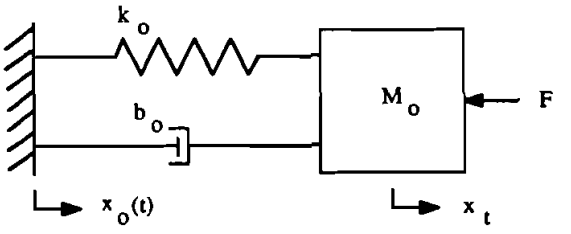

Figure 18. Target system.

The results are $K = -91$ and $B = -1{\cdot}86$—notably this approach encourages a significant departure from servo philosophy: we are using positive feedback to add negative stiffness and negative damping (a direct result of our concern with interactive behaviour). These values fall within the acceptable region of the $K-B$ plane shown in Fig. 17, guaranteeing coupled and uncoupled stability.

Performance may be evaluated in the frequency domain by comparing the command-following and driving-point impedance Bode plots of the controlled manipulator and the target system. The Bode plots of $x_2(s)/x_0(s)$ and $x_t(s)/x_0(s)$ are shown in Fig. 19. Although no quantitative standard of evaluation has been

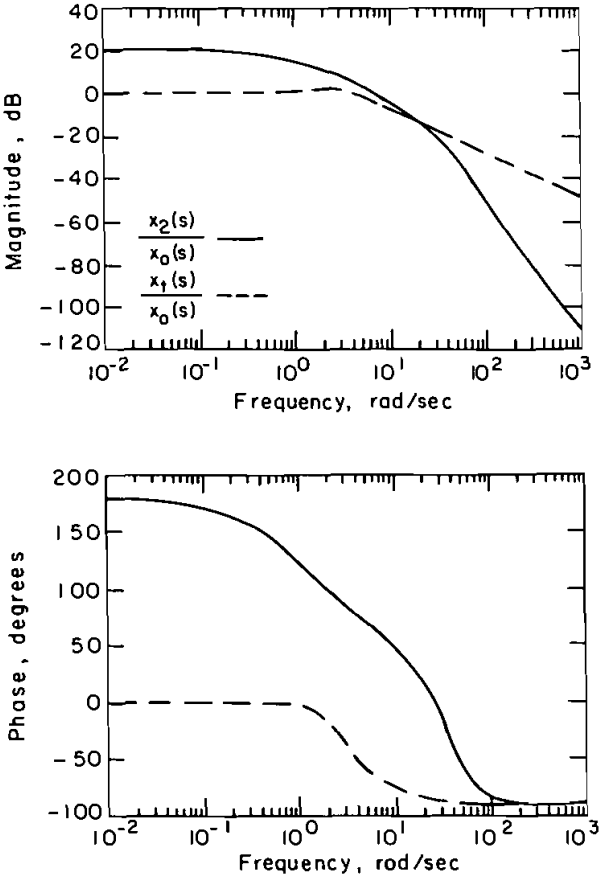

Figure 19. Command-following performance.

established, it is clear that the command-following of the manipulator is not very good.

The Bode plots of $v_2(s)/F(s)$ and $v_t(s)/F(s)$ are shown in Fig. 20. The interactive behaviour is promising at low and high frequencies, but shows a significant departure from that of the target system in the middle range.

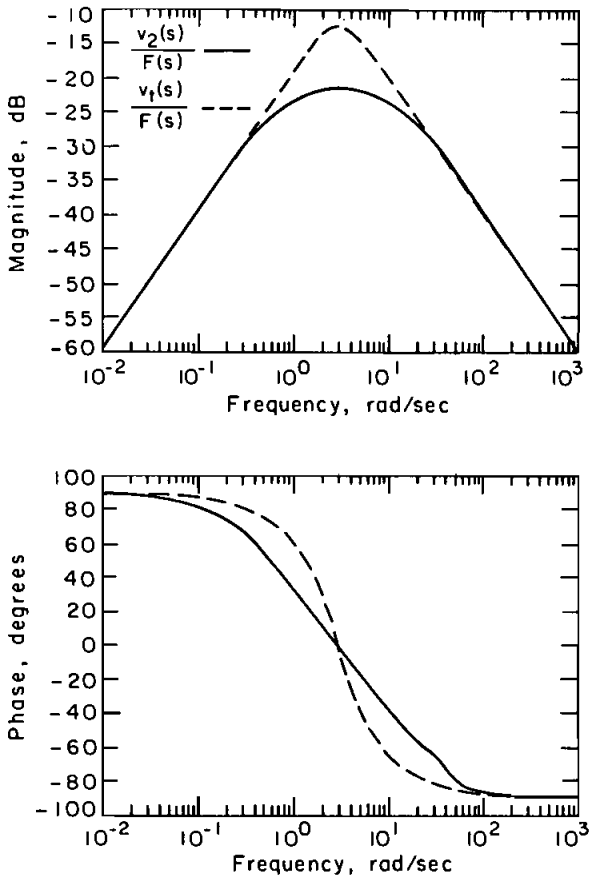

Figure 20. Interactive behaviour performance.

The point of this analysis has been that to ensure coupled stability is possible given a particular control law, but that this does not necessarily constitute an effective design procedure. In § 7 a technique that attempts to satisfy both stability and performance specifications will be considered.

As suggested in § 5, an alternative method based on the root locus may also be used to investigate the coupled stability properties of a particular closed-loop system. Two root loci are needed, one which describes coupling to all springs and one which describes coupling to all masses. This method may also be used to examine performance, simply by comparing the results with those obtained with the target system.

The results for the closed-loop system considered in this section are shown in Figs. 21 and 22. As expected, the coupled system is stable for all values of k_{env} and M_{env}, but there is a significant disparity between the behaviour of the actual and target systems.

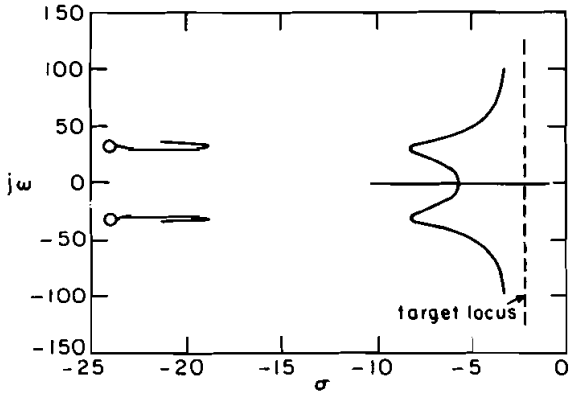

Figure 21. Locus of poles when coupled to springs.

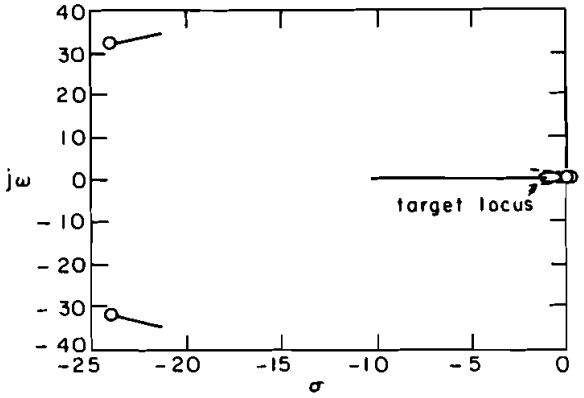

Figure 22. Locus of poles when coupled to masses.

7. Achieving target behaviour—a linear example

The purpose of this section is to demonstrate one systematic approach to the design of an interaction controller which addresses both stability and performance requirements.

We begin with a foray into non-linear controller design. Assume that we have a non-linear manipulator which may be described by equations in the same canonical form as that used in § 6, i.e.

$$\left.\begin{aligned} \dot{x}_1 &= v_1 \\ \dot{x}_2 &= v_2 \\ \dot{v}_1 &= f_1(x_1, v_1, x_2, v_2, E) \\ \dot{v}_2 &= f_2(x_1, v_1, x_2, v_2, F) \end{aligned}\right\} \tag{7.1}$$

As before, x_1 and v_1 correspond roughly to actuator and transmission states, and x_2 and v_2 correspond roughly to hardware (linkage) states. E is the control input, and F is an environmentally imposed force. We also define a non-linear target model which contains no actuator or transmission dynamics and is, therefore, of lower order than

the manipulator model

$$\left.\begin{aligned}\dot{x}_t &= v_t \\ \dot{v}_t &= f_t(x_t, v_t, x_0, v_0, F)\end{aligned}\right\} \tag{7.2}$$

x_0 and v_0 represent the virtual trajectory, and F is the environmental force. One way of deriving a control law is to equate the motion of the manipulator to that of the target model:

$$x_2 = x_t \tag{7.3}$$

$$v_2 = v_t \tag{7.4}$$

$$f_2(x_1, v_1, x_2, v_2, F) = f_t(x_2, v_2, x_0, v_0, F) \tag{7.5}$$

Equations (7.4) and (7.5) represent successive differentiations of (7.3), which defines the desired behaviour. There are various paths from which to choose. For instance, (7.5) may be differentiated again, as often as is necessary, to expose the control E. E could then, presumably, be solved to yield a control law.

There are problems with this approach however. One is simply that it may not be possible to solve explicitly for E. Another problem is that implementing a particular control law does not guarantee that the equation which was differentiated to obtain it is implemented—there is an arbitrary constant of integration that occurs in the reverse process. Typically, this results in behaviour much like that caused by a pole at the origin—slow drift. For instance, if we succeed in implementing $v_2 = v_t$, then $x_2 = x_t$ is not guaranteed; the values are likely to drift apart. Of course, multiple differentiations exacerbate the problem.

As an aside, sliding mode control (Slotine and Sastry 1983) is a technique which ensures that the constant of integration is (on average) zero. However, it works only when the desired behaviour and the control law are separated by a single differentiation; the authors know of no technique that may be used when multiple differentiations are needed to derive the control law.

The problem of the constants of integration is a difficult one, and we do not attempt to deal with it here. However, rather than making matters worse by differentiating (7.5) again, this equation will be taken as a prescription for a servo design. That is, we require that f_t be of such a form that we may separate the virtual trajectory terms and write

$$f_2(x_1, v_1, x_2, v_2, F) - f_{t0}(x_2, v_2, F) = f_{t1}(x_0, v_0) \tag{7.6}$$

The left side of this equation may be taken to define the output of a servo, and the right side the input, and we may use any available servo design technique to implement it. Notice that the technique requires, in general, the use of full-state feedback as well as the measurement of interaction port variables such as the force applied to the manipulator.

This technique may be applied to the linear manipulator and target model of § 6. The result is the following equation

$$\left[\frac{k_1}{M_2}\right]x_1 + \left[\frac{k_1}{M_t} - \frac{k_1 + k_2}{M_2}\right]x_2 + \left[\frac{b_t}{M_t} - \frac{b_2}{M_2}\right]v_2 + \left[\frac{1}{M_2} - \frac{1}{M_t}\right]F = \left[\frac{k_t}{M_t}\right]x_0 + \left[\frac{b_t}{M_t}\right]v_0 \tag{7.7}$$

For the particular parameter values chosen in § 6, (7.7) reduces to

$$160x_1 - 251x_2 - 1{\cdot}76v_2 = 9x_0 + 4{\cdot}2v_0 \tag{7.8}$$

Almost certainly, the simplest method of implementing this equation is to use classical control techniques to design a proportional controller, as shown in Fig. 23.

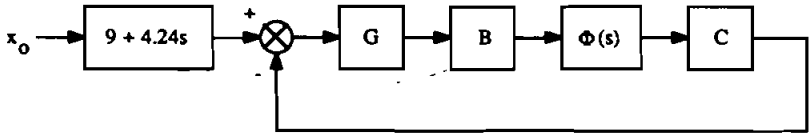

C = [160 -251 0 -1.76]

Figure 23. Block diagram of interaction controller design.

One advantage of this technique is that it allows us to use a single parameter, G, to describe the allowable spaces for uncoupled and coupled stability. Another, more sophisticated, technique that provides this same advantage is the so-called 'cheap control' LQR design (Kwakernaak and Sivan 1972), which reduces the design

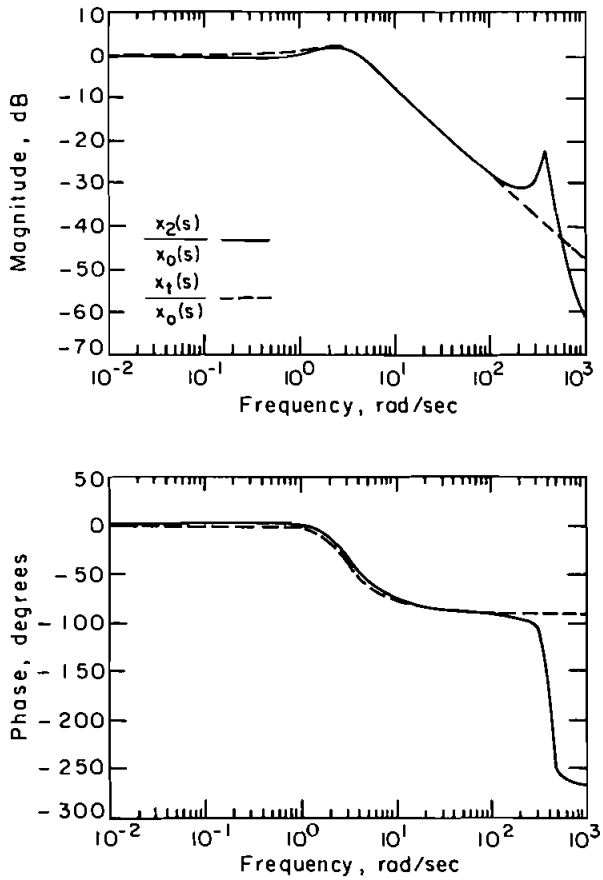

Figure 24. Command-following performance.

problem to the selection of a single parameter, the control weighting on the cost functional. An LQR design would even provide a guarantee of uncoupled stability. The technique is, however, very poorly suited to a situation in which environmental disturbances are present, as it requires a backwards integration from $t = \infty$ (presumably the disturbances are unknown in the future), so that in the general case in which measurements of port variables are required it would not be useful.

Getting back to the problem at hand, the values of G for which coupled and uncoupled stability are guaranteed may be found. The results are:

Uncoupled stability: $G \geqslant -0{\cdot}848$

Coupled stability: $G \geqslant -0{\cdot}737$

There is no upper bound on G, which means that for this problem we may come arbitrarily closd to matching both the command following and interactive behaviour of the target model. Of course, actuator limitations provide practical limits on the value of G.

Figures 24 and 25 show the manipulator performance for $G = 100$ in terms of Bode plot comparisons with the target model. In this case, both the command following and the interactive behaviour are excellent. As might be expected, roll-off and accompanying phase lag limit the command-following bandwidth. There is, however, no

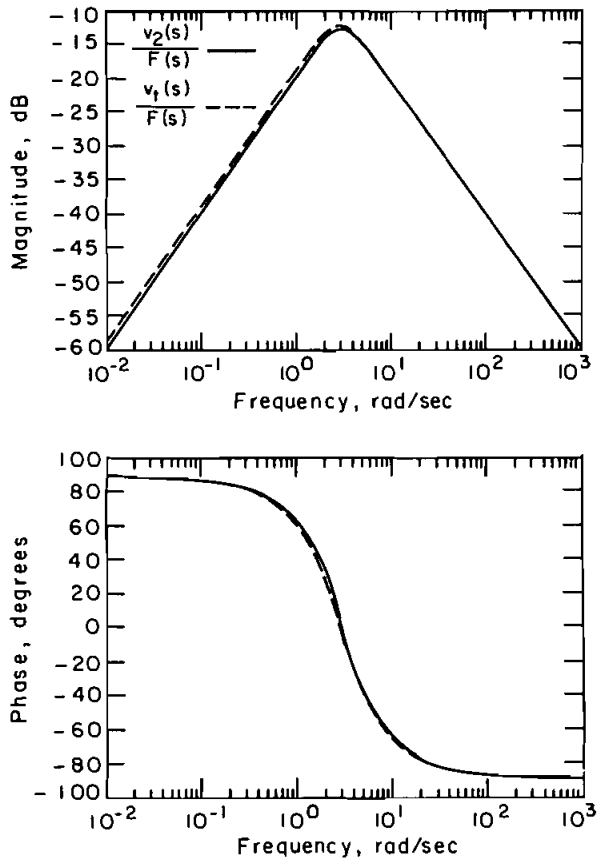

Figure 25. Interactive behaviour performance.

bandwidth limitation on the interactive behaviour. This is primarily due to the selection of a target model sufficiently similar to the manipulator model. Both models include a unity mass at the environmental interaction port, and this mass is principally responsible for the driving-point behaviour at high frequency.

Figures 26 and 27, which show the root locus test for coupled stability, support the conclusion regarding interactive behaviour. Figure 26 shows the most improvement; for the same range of values of k_{env} used in Fig. 21, this root locus is indistinguishable from that of the target system.

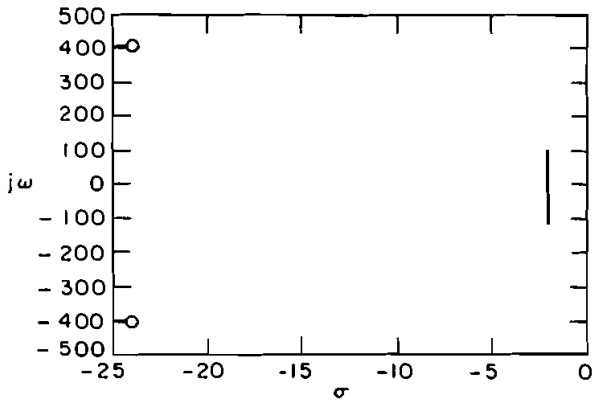

Figure 26. Locus of poles when coupled to springs.

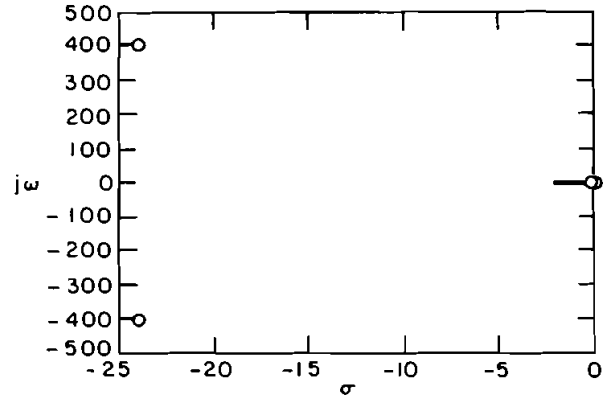

Figure 27. Locus of poles when coupled to masses.

8. Conclusions

This paper has addressed the problem of designing interaction controllers—a problem that arises in the study of manipulation. In particular, we are interested in expanding the repertoire of tasks which a robotic manipulator may perform, by controlling its interactive behaviour. Towards this end, an approach to the design of manipulator controllers which differs from a servo approach in its attention to interactive behaviour has been proposed. The significant results developed in this paper may be summarized as follows.

(i) The approach to designing 'interaction controllers' is significantly different from the approach to servo design in that it includes specifications for coupled stability and interactive behaviour.

(ii) A necessary and sufficient condition to guarantee the stability of a linear system coupled to a passive hamiltonian environment is that the driving point impedance of the linear system be positive real.

(iii) The stability guarantee holds for active linear environments as well, provided that the environment may be described as a passive system with state-independent control.

(iv) For any linear system, the 'worst' linear environment is some set of springs or masses. These may be found with a root locus technique.

(v) The positive real condition may be used to place bounds on control gains in order to guarantee the coupled stability of a closed-loop design. An example has been provided.

(vi) A linear design example which results in both a guarantee of coupled stability and desirable interactive behaviour (defined in terms of a target model) has been presented.

Future work will include similar analyses of more sophisticated manipulator models and design techniques, as well as experimental interrogation of the analysis. This style of analysis is currently being used to investigate the effects of force feedback on the coupled stability properties of a manipulator. Finally, the role of other design specifications, such as robustness measures, will be investigated.

Appendix A

Driving-point impedances

The following are the necessary and sufficient conditions for $Z(s)$ to qualify as a driving-point impedance for a passive system (Brune 1931).

(i) $Z(s)$ is a rational function of the complex frequency variable $s = \sigma + j\omega$ and is analytic in general.

(ii) $\text{Re}\{Z(s)\} \geqslant 0$ for $\text{Re}\{s\} \geqslant 0$.

(iii) $Z(s)$ is real when s is real.

Some of the corollaries of these conditions are as follows.

(*a*) $Z(s)$ is a ratio of two polynomials in s with real coefficients.

(*b*) The poles and zeros of $Z(s)$ are restricted to the $j\omega$ axis and to the LHP.

(*c*) Any poles which are not real must occur in complex conjugate pairs.

(*d*) The poles on the $j\omega$ axis (including those at 0 and ∞) are simple with positive-real residues, i.e. for a pole at $j\omega_1$:

$$\lim_{s \to j\omega_1} [Z(s)(s - j\omega_1)] \geqslant 0$$

(*e*) The zeros on the $j\omega$ axis (including those at 0 and ∞) are simple with positive differential quotients, i.e. for a zero at $j\omega_2$:

$$\lim_{s \to j\omega_2} \left[\frac{Z(s)}{s - j\omega_2} \right] \geqslant 0$$

Appendix B

In this appendix, it is shown that a Nyquist plot which contains a counterclockwise loop (such as those in Figs. 5 *d*, *e*) represents a transfer function with at least one RHP pole. Transfer functions of the following form will be considered

$$A(s) = \frac{\alpha_0 s^m + \alpha_1 s^{m-1} + \ldots + \alpha_m}{s^n + \beta_1 s^{n-1} + \ldots + \beta_n} \tag{B 1}$$

where $m \leqslant n$. N will refer to the number of clockwise encirclements of the origin by the Nyquist plot of $A(s)$, P to the number of RHP poles of $A(s)$, and Z to the number of RHP zeros of $A(s)$. There are two cases:

Case 1

This is the trivial case in which the counterclockwise loop encircles the origin; therefore

$$Z - P = -1 \tag{B 2}$$

Clearly, as $Z \geqslant 0$, it is necessary that $P \geqslant 1$.

Case 2

This is the general case in which the counterclockwise loop does not encircle the origin: therefore

$$Z - P = 0 \tag{B 3}$$

In this case, we find some point $a + bj$ which is encircled by the loop, and consider a mapping of the Nyquist contour through $A(s) - (a + bj)$. This mapping has a shape identical to that of $A(s)$, but is shifted so that the loop now encircles the origin. Furthermore, it is evident that $A(s)$ and $A(s) - (a + bj)$ share the same poles

$$A(s) - (a + bj) = \frac{(\theta_0 + \varphi_0 j)s^n + (\theta_1 + \varphi_1 j)s^{n-1} + \ldots + (\theta_n + \varphi_n j)}{s^n + \beta_1 s^{n-1} + \ldots + \beta_n} \tag{B 4}$$

For the shifted transfer function, the Nyquist plot reveals

$$Z' - P = -1 \tag{B 5}$$

or

$$P = Z' + 1 \geqslant 1 \tag{B 6}$$

This completes the proof. □

ACKNOWLEDGMENTS

This work was supported in part by grants from the National Science Foundation (Nos. ECS-8307461 and EET-8613104) and from the National Institute of Disabilities and Rehabilitation Research, US Department of Education (No. G000830074).

REFERENCES

BRUNE, O., 1931, *J. Math. Phys., M.I.T.*, **10**, 131.

FASSE, E. D., 1987, Stability robustness of impedance controlled manipulators coupled to passive environments. S.M. thesis, M.I.T., Cambridge, Mass.

HOGAN, N., 1984, Some Computational problems simplified by impedance control. *ASME Conf. on Computers in Engineering*, Las Vegas; 1985 a, *J. dynam. Syst. Meas. Control*, **107**, 1; 1985 b, *Ibid.*, **107**, 8; 1985 c, *Ibid.*, **107**, 17; 1985 d, Control strategies for complex movements derived from physical systems theory. *Complex Systems—Operational Approaches in Neurobiology, Physics, and Computers*, edited by H. Haken, *Proc. Int. Symp. on Synergetics*, Schloß Elmau, Bavaria (Berlin: Springer-Verlag).

KWAKERNAAK, H., and SIVAN, R., 1977, *Linear Optimal Control Systems* (New York: Wiley-Interscience).

LEHTOMAKI, N. A., 1981, Practical robustness measures in multivariable control. Ph.D. thesis, M.I.T., Cambridge, Mass.

PAYNTER, H. M., 1961, *Analysis and Design of Engineering Systems* (Cambridge, Mass.: M.I.T. Press).

ROSENBERG, R. C., and KARNOPP, D. C., 1983, *Introduction to Physical Systems Dynamics* (New York: McGraw-Hill).

SLOTINE, J.-J. E., and SASTRY, S. S., 1983, *Int. J. Robotics Res.*, **38**, 465.